Population Pharmacokinetics of Liposomal Amphotericin B in Immunocompromised Children

Running Title: Pharmacokinetics of liposomal amphotericin in children

Jodi M. Lestner[1], Andreas H. Groll[2], Ghaith Aljayyoussi[3], Nita L. Seibel[4,5], Aziza Shad[6], Corina Gonzalez[7], Lauren V. Wood[8], Paul F. Jarosinski[9], Thomas J. Walsh[4,10-12], and William W. Hope[1]

1 Antimicrobial Pharmacodynamics and Therapeutics, University of Liverpool, UK

2 Center for Bone Marrow Transplantation and Department of Pediatric Hematology/Oncology, University Children's Hospital Münster, Münster, Germany

3 Liverpool School of Tropical Medicine, UK

4 Immunocompromised Host Section, Pediatric Oncology Branch, National Cancer Institute, Bethesda, MD, USA

5 Children's National Medical Center and George Washington University School of Medicine and Public Health, Washington, DC, USA

6 Clinical Investigations Branch, Cancer Treatment Evaluation Program, National Cancer Institute, Bethesda, MD, USA

7 Department of Pediatrics, Division of Pediatric Hematology/Oncology, Georgetown University Medical Center, Washington, DC, USA

8 Center for Cancer Research, National Cancer Institute, Bethesda, MD, USA

9 Pharmacy Department, National Institutes of Health Clinical Center, Bethesda, MD, USA

10 Transplantation-Oncology Infectious Disease Program, Weill Cornell Medical Center, NY, USA

11 Department of Pediatrics, Weill Cornell Medical Center, NY, USA

12 Department of Microbiology, Weill Cornell Medical Center, NY, USA

Corresponding Author: Dr Jodi Lestner

Antimicrobial Pharmacodynamics and Therapeutics

1.09 Sherrington Building

Ashton Rd

University of Liverpool

Liverpool L69 3GE

Telephone +44 (0)151 794 5941

Email: jlestner@liverpool.ac.uk

Conflicts of Interest

WWH has acted as consultant, received research support for Merck, Pfizer Inc., Astellas, Gilead Sciences, F2G.

TJW receives research grants for experimental and clinical antimicrobial pharmacotherapeutics from Astellas, Novartis, Merck/Cubist, Pfizer, and Theravance. He has served as consultant to Astellas, Merck/Cubist, Contrafect, Novartis, Pfizer, and Methylgene.

AHG has received research grants from Gilead and Merck, Sharp & Dohme, and Pfizer; is a consultant to Astellas, Basilea, Gilead, Merck, Sharp & Dohme, and served at the speakers´ bureau of Astellas, Basilea, Gilead, Merck, Sharp & Dohme, Pfizer, Schering-Plough and Zeneus/Cephalon.

JML, GA, NS, AS, IB, CG, LVW, PFJ none declared.

Keywords

Liposomal, amphotericin B, children, pediatrics, pharmacokinetics, invasive fungal disease

Abstract

Background Liposomal amphotericin B (LAmB) is widely used in the treatment of invasive fungal disease (IFD) in adults and children. There are relatively limited PK data to inform optimal dosing in children that achieves systemic drug exposures comparable to those of adults.

Objectives To describe the pharmacokinetics of LAmB in children aged 1-17 years with suspected or documented IFD.

Methods Thirty-five children were treated with LAmB at dosages of 2.5-10 mg kg^{-1} daily. Samples were taken at baseline and at 0.5-2.0 hourly intervals for twenty-four hours after receipt of the first dose (n=35 patients) and on the final day of therapy (n=25 patients). LAmB was measured using high performance liquid chromatography (HPLC). The relationship between drug exposure and development of toxicity was explored.

Results An evolution in PK was observed during the course of therapy resulting in a proportion of patients (n=13) having significantly higher maximum serum concentration (C_{max}) and area under the concentration time curve (AUC_{0-24}) later in the course of therapy, without evidence of drug accumulation (C_{min} accumulation ratio, AR < 1.2). The fit of a 2-compartment model incorporating weight and an exponential decay function describing volume of distribution best described the data. There was a statistically significant relationship between mean AUC_{0-24} and probability of nephrotoxicity (OR 2.37; 95% CI 1.84-3.22, p=0.004).

Conclusions LAmB exhibits nonlinear pharmacokinetics. A third of children appear to experience a time-dependent change in PK, which is not explained by weight, maturation or observed clinical factors.

Introduction

The small unilamellar liposomal formulation of amphotericin B (LAmB; AmBisome®) is widely used for the treatment of invasive fungal disease (IFD) in adults and children. This compound has been available for over two decades and is a first line agent in the treatment of serious opportunistic diseases that include invasive aspergillosis, invasive candidiasis, cryptococcal meningoencephalitis, and mucormycosis. (1-4)

Despite extensive clinical experience, many of the details relating to the underlying pharmacological properties of LAmB remain unclear. A limited number of datasets and population pharmacokinetic (PK) models have been reported for LAmB. (5-7) These analyses were based on data gathered from patients receiving relatively low dosages and exclusively sampled early in the course of therapy. There are very limited data reporting the PK of LAmB in pediatric populations.

A better understanding of the pharmacological properties of LAmB remains a priority and would enable optimal dosing, particularly for special populations such as infants and children. Dosages ranging from 2.5-10 mg kg^{-1} per day were studied and each patient was intensively sampled. The individual PK profiles for a sub-population of participants (n=25) were compared at the commencement and end of therapy.

Materials & Methods

Patients, Antifungal Regimen

This study was designed as a prospective, multi-center, open-label phase II clinical trial. Study protocol approval was obtained from the Ethics Committees of the National Cancer Institute (Bethesda MD, USA); Children's National Medical Center (Washington DC, USA) and Georgetown University Medical Center (Washington DC, USA). Informed consent was obtained prior to enrolment in each case. A total of 35 children with a diagnosis of confirmed or suspected IFD were enrolled. Patients received LAmB infused over one hour at dosages of 2.5, 5.0, 7.5, or 10.0 mg kg^{-1} daily (n= 9, 13, 8, and 8, respectively). Two patients received LAmB as treatment for more than one discrete clinical episode requiring antifungal therapy. Patients undergoing multiple discrete episodes were assigned the same identification number on each occasion and were handled using the dosing reset function in Pmetrics.

LAmB (AmBisome®; Gilead Sciences, Inc., Foster City, California) was supplied as a lyophilized powder and stored at 2-8°C until use. Powder (50 mg) was reconstituted with 12.5 mL of sterile water to a concentration of 4 mg^{-1} mL, and then further diluted in 5% dextrose. Reconstituted drug was used within 6 hours.

Pharmacokinetic Sampling

PK samples were obtained on the first and last day of therapy. The first day of LAmB administration was defined as day one. Heparinized whole-blood samples (0.6-1 mL) were collected by peripheral intravenous catheter. Samples were obtained prior to administration, and at 0.5-2.0 hourly intervals for 24 hours following the start of each infusion. A total of 7-12 samples were obtained per patient within each sampling period (total sampling blood volumes < 3 mL/kg within 24 hours). Sampling was repeated in sixteen patients on the last

115 day of therapy (12-41 days) using the same sampling schedule. Plasma fractions were
116 separated by centrifugation at 1,500 g for 10 min at 4°C and stored at −80°C until analysis.

117 Concentrations of LAmB in plasma were determined by a high-performance liquid
118 chromatographic assay. (8) Briefly, total active drug and internal standard, 3-nitrophenol,
119 were extracted in methanol and separated by reversed-phase chromatography. The separation
120 was performed isocratically using a Supelcosil ABZ+Plus analytical column (3 μm particle
121 size, 150 mm x 4.6 mm internal diameter; Supelco, Bellefonte, Pennsylvania), coupled by a
122 Keysone C18 guard column (3 μm particle size, 7.5 mm x 4.6 mm 7.5 by 4.6 mm; Western
123 Analytical, Murrieta, California). The mobile phase, consisting of 10 mM sodium acetate
124 buffer, including 10 mM EDTA (pH 3.6) and acetonitrile (650:350, vol/vol), was delivered at
125 a flow rate of 1.0 ml/min using a Spectra-Physics Model 250 pump (Thermo Separations, San
126 Jose, California). UV absorbency peaks were detected at a wavelength of 406 nm using a
127 Waters Model 440 UV-VIS detector (Waters Corp, Milford, Massachusetts). Two
128 overlapping standard curves were used: 0.05 to 20 μg/ml and 0.5 to 200 μg/ml. The assay was
129 linear over a range of 0.05-20 and 0.5 to 200 μg/mL (r^2 >0.995). Intra- and inter-day
130 coefficients of variation were 9.5 and 7.0%, and 5.4 and 6.0%, respectively, and the limit of
131 quantification was 0.05 μg/ml. The average recovery was 90.5% at the concentrations of
132 quality control samples with a standard deviation of 6.2%.

133

134 ***Population Pharmacokinetic Modeling***

135 Data were analysed using a non-parametric methodology within the program Pmetrics
136 (version 1.2.6; University of Southern California, Los Angeles, CA). (9) The observed data
137 were weighted using the inverse of the estimated assay variance.

Structural models were constructed and used to fit patient data. One-, two- and three-compartment models with zero-order drug input into the central compartment and both first-order and nonlinear (Michaelis-Menten) elimination from the central compartment were explored. A proportion of patients had concentration-time profiles that indicated an intra-individual change in PK during the course of therapy (n=13; 52%). Affected individuals demonstrated a marked increase in excursion of drug concentrations from C_{max} to C_{min} and a disproportionate increase in $AUC_{0\text{-}24}$ (Figure 1). This change was not associated with rising trough concentrations, suggesting the phenomenon did not result from drug accumulation resulting from conventional nonlinear (Michaelis-Menten) kinetics (AR <1.2). Inspection of the data suggested the clearance of drug was the same in both sampling periods. Hence, the following structural model that allowed Vd to change with time was explored. In this model, volume contracted with time and was described using an exponential decay function. Clearance (Cl) was scaled according to weight using a standard 0.75 power function. The differential equations describing the final model were as follows:

$$\frac{\delta X(1)}{\delta t} = R(1) - (Cl * (\frac{wt}{70})^{0.75}/Vd) * X(1) - Kcp * X(1) + Kpc * X(2)$$

$$\frac{\delta X(2)}{\delta t} = Kcp * X(1) - Kpc * X(2)$$

$$\frac{\delta Vd}{\delta t} = -Vin * K + Vfin$$

Where: X(1) and *X*(2) represent the total (bound and free) amount of LAmB (mg) in the central (*c*) and peripheral (*p*) compartments, respectively. *R*(1), *K*cp and *K*pc represent the rate of infusion into the central compartment (mg h^{-1}) and first-order inter-compartmental rate constants, respectively. Clearance (Cl) is normalised according to a 70 kg individual and allometrically scaled. The volume of the central compartment (Vc) is described by an

158 exponential decay function in which initial volume (Vin) reduced over time according to a
159 rate constant (K) to a final volume (Vfin).

160 The goodness-of-fit of each model to the data was assessed by visual inspection of the
161 observed-predicted values and following linear regression of the observed-predicted values
162 both before after the Bayesian step. The coefficient of determination (r^2), slope and intercept
163 of each regression were calculated. Statistical comparison of models was based on likelihood
164 ratio, in which twice the likelihood difference was evaluated against a $\chi 2$ distribution with an
165 appropriate number of degrees of freedom. In addition, predictive performance was assessed
166 according to weighted-mean error (a measure of bias) and bias-adjusted weighted-mean-
167 squared error (a measure of precision).

168 The final selected model was validated using a nonparametric bootstrap resampling
169 technique. Three hundred bootstrap datasets were constructed based on random sampling
170 with replacement using ADAPT 5. Measures of central tendency and dispersion and the 95%
171 confidence interval (CI) for each parameter value were calculated and compared with
172 estimates from original data. The selected structural model was then implemented within the
173 simulation module of ADAPT 5. (10) Bayesian estimates of the PK parameters for each
174 patient were used to calculate simulated peak plasma concentration (C_{max}), trough plasma
175 concentration (C_{min}), and area under the concentration time curve over 24 hours (AUC_{0-24}) at
176 defined therapeutic time points.

177 Potential relationships between measures of drug exposure (C_{max}, C_{min}, absolute
178 LAmB dosage, weight adjusted dosage, $AUC_{0-24,}$ and mean AUC_{0-24}) and toxicity were
179 explored. Toxicity was defined as changes from baseline values at commencement of therapy
180 as follows: nephrotoxicity as an increase in serum creatinine (SCr) of $\geq$0.5 mg/dL or
181 doubling of baseline value, hypokalemia as a fall in potassium of $\leq$3.0 mmol/L or $\geq$50% from

baseline, anemia as an hemoglobin of ≤8.0 g/dL, and hepatotoxicity as a rise in bilirubin by ≥1.5 mg/dL or AST or ALT ≥3 times above baseline. A conservative definition was used to define change in biological parameters in order to overcome variability in sampling between patients; pre-treatment value was subtracted from the highest measurement observed for each patient during the treatment course.

Results

The patient demographics of the study cohort are summarized in table 1. The mean ± SD weight was 26.9 ± 14.0 kg with a range of 8.8-67.5 kg. There was wide variability in the duration of therapy: the mean ± SD was 11.9 ± 9.41 days of therapy with a range of 1-41 days. The most common underlying diagnosis was hematological malignancy (n =21). Nine patients had undergone allogeneic hematopoietic stem-cell transplantation (HSCT) and 23 received concomitant antineoplastic chemotherapy. The majority of patients received LAmB as empirical therapy for suspected IFI (n=31). Seven patients received treatment for confirmed IFI. There were two cases of invasive aspergillosis due to A. *fumigatus*, and a further case that developed during treatment with LAmB that was classified as a breakthrough infection. Three patients had invasive candidiasis: one central-line infection and one severe oesophagitis due to C. *albicans*, and one case of candidaemia caused by C. *parapsilosis*. There was a single case of cryptococcal meningoencephalitis complicating HIV infection. Clinical success was defined according to clinical, radiological, and mycological response during the study period plus relapse-free survival at 2 months after the end of therapy. Clinical success was reported in 76% of probable (n=29) and 43% (n=3) of proven fungal infections.

205 The Bayesian estimates for clearance (Cl) obtained from standard two-compartment models
206 for each patient were plotted against weight. A relationship between the log_{10}-transformed
207 estimates was apparent. The performance of models incorporating an allometric power
208 function was therefore investigated using a scaling exponent fixed at 0.75. No significant
209 relationship was found between Bayesian estimates for volume (Vd) and weight. Differences
210 in clinical factors that might be predicted to alter the PK of LAmB were explored. No
211 significant differences were identified in liver function, serum albumin, white blood cell
212 (WBC) count and total protein concentrations, use of parenteral nutrition and concomitant
213 steroids. A relatively poor fit of standard model structures was apparent (see, for example
214 performance of a standard two-compartment model, figure 2). Conventional compartmental
215 model structures failed to account for the widening excursion of drug concentrations
216 observed in a portion of patients. The parameter estimates for the base and final model are
217 summarized in table 2. The fit of the selected model incorporating a function describing
218 contraction in Vd was satisfactory ($r^2 = 0.90$), and compared favourably to a standard 2-
219 compartment model. The final model consisted of eight support points. Measures of bias and
220 precision were acceptable (see figure 2). The bootstrap mean and 95% CI values for
221 parameters closely approximated the estimates obtained from the final model (table 3),
222 indicating that the parameter estimates from the final model were robust. Both the mean and
223 median parameter values resulted in comparable intercept, slopes and overall r^2 values. The
224 log-likelihood value for the final model was significantly better (more positive) than for the
225 standard 2-compartment model ($\chi^2 = 48.95$, $p = <0.001$). Figure 3 shows the simulated
226 concentration-time profiles and raw data for two examples of patients that exhibited time-
227 dependent and time-independent changes in PK profiles.

228 Dose-exposure relationships were further explored. No correlation between absolute
229 dose and exposure (C_{max}, C_{min} or AUC_{0-24}) was observed, an expected finding given the

significant variability in weight within the study population. Significant relationships between dose per-unit-weight and exposure were observed. Plots of dose-normalized C_{max} and AUC_{0-24} suggest nonlinearity (figure 4), although a dosing threshold associated with a discrete change in exposure was not observed.

Transient renal impairment and hypokalemia were common, occurring in 46% (n=16) and 23% (n=8) of patients, respectively. A significant correlation between steady state exposure (AUC_{0-24}) and change in serum creatinine (ΔSCr) was observed (Figure 5, r=0.594, p=0.015). A statistically significant relationship between mean AUC_{0-24} and probability of developing nephrotoxicity (OR 2.37; 95% CI 1.84-3.22, p=0.004). There was insufficient clinical information to explore the impact of other potential determinants of renal impairment (for example disease severity and concomitant nephrotoxic drugs) in this study cohort. No significant correlations were found between LAmB exposure (in terms of absolute dose, weight adjusted dose, AUC_{0-24} or mean AUC_{0-24}) and other toxicity including hypokalemia, anemia, and hepatotoxicity.

Discussion

Liposomal amphotericin B is used extensively for the treatment of IFD. Dosages of 3-6 mg kg^{-1} are approved in the U.S.A and the E.U. in both adults and children. These dosages are not based on an in-depth knowledge of the pharmacology of the drug, but rather results from preclinical in vivo studies and clinical trials that have attempted to identify regimens that appear safe and effective. There continues to be considerable uncertainty regarding the lowest effective dosage of LAmB that achieves adequate antifungal effect. As a result, dosages of 1-15 mg kg^{-1} have been studied in a range of clinical settings including

253 empirical therapy, invasive aspergillosis, invasive candidiasis, and cryptococcal
254 meningoencephalitis. (11-14)

255 Phase I/II clinical studies of LAmB in children and adults have highlighted variable,
256 dose-dependent PK. Children and adults receiving LAmB at conservative daily doses of 1-3
257 mg kg^{-1} exhibit linear PK that are described by standard two- or three-compartment models
258 with first-order elimination. (6, 7)(5) Limited data suggest nonlinearity at higher dosages.
259 Walsh *et al.* observed time-dependent nonlinear PK and an apparent paradoxical dose-
260 dependent exposure plateau in adults receiving daily dosages of 7.5-15 mg kg^{-1}. (3) The data
261 from paediatric patients in this study similarly suggests that a proportion of patients exhibit
262 time-dependent nonlinear PK. When the concentration-time profiles of patients exhibiting
263 nonlinear PK are examined a significant excursion in C_{min}-C_{min} is observed, a change not
264 associated with a proportional increase in half-life that would be expected with classical
265 nonlinear (Michaelis-Menten) clearance, but rather appears to reflect a contraction in the
266 volume of distribution during the course of therapy. Whereas the limited data from adults has
267 suggested a paradoxical dose-dependent reduction in exposure at doses >7.5 mg kg^{-1}, in
268 children higher doses appear to be associated with an increased probability of nonlinearity.
269 The reason for this difference is unclear and warrants further study.

270 High-density lipoproteins (HDL) mediated opsonization of lipid formulations of
271 amphotericin B within plasma has been shown to drive uptake into mononuclear phagocytes
272 and deposition within the liver and spleen. (15-18) Hong *et al.* reported a negative correlation
273 between Bayesian estimates volume of distribution and the fraction of HDL-associated
274 LAmB in 21 children and adolescence receiving LAmB at daily doses of 0.8-6 mg kg^{-1}. We
275 hypothesize that variable HDL saturation and/or phagocyte uptake may be the
276 pathophysiological processes driving the inter-individual variability observed in this study.
277 However, many patients in this small clinical cohort exhibited significant fluctuations in

hematological parameters such as WBC count over the course of antifungal therapy, primarily due to underlying hemato-oncological diagnoses, and we were not able to further characterise relationships between specific hematological parameters and volume contraction. Other significant data such as plasma HDL concentrations were not quantified in this study. This is an interesting hypothesis that warrants further study in experimental models and/or as part of larger clinical trials. LAmB is generally well tolerated with a significantly improved toxicity profile when compared to conventional amphotericin B deoxycholate. (14) Dosages of LAmB as high as 15 mg kg^{-1} daily have been reportedly well tolerated in adults. (3) A number of studies including one large RCT have, however, described dose-dependent toxicity with significantly higher rates of renal impairment and hypokalemia at dosages at or above 10 mg kg^{-1} daily. (1) In this study, a significant proportion of patients developed transient renal impairment and/or hypokalemia during the course of treatment. In view of the limited data available, significant inter-individual variability and lack of obvious inflection point in this relationship further analysis to define exposure thresholds was not possible. The correlation between drug exposure and ΔSCr observed here suggests, however, that clinical vigilance and assiduous monitoring of renal function is required to minimize the probability of toxicity associated with LAmB.

Taken together these data suggest that a significant proportion of pediatric patients receiving LAmB at daily doses > 5.0 mg kg^{-1} exhibit nonlinear PK with significantly higher peak concentrations and overall drug exposure. This phenomenon was not predicted by clinical covariates quantified in this study. Therapeutic drug monitoring (TDM) is thus likely to be of value in identifying this subpopulation in order to prevent toxicity. Effective implementation of TDM would require a more detailed understand of exposure-toxicity relationships and data describing disease severity in children with proven or probably IFD in order to define target exposure thresholds.

Acknowledgements

None declared.

Funding

This study received funding from Astellas Pharma US, Inc..

References

1. **Cornely OA, Maertens J, Bresnik M, Ebrahimi R, Ullmann AJ, Bouza E, Heussel CP, Lortholary O, Rieger C, Boehme A, Aoun M, Horst HA, Thiebaut A, Ruhnke M, Reichert D, Vianelli N, Krause SW, Olavarria E, Herbrecht R, AmBiLoad Trial Study G.** 2007. Liposomal amphotericin B as initial therapy for invasive mold infection: a randomized trial comparing a high-loading dose regimen with standard dosing (AmBiLoad trial). Clinical infectious diseases : an official publication of the Infectious Diseases Society of America **44:**1289-1297.
2. **Ellis M, Spence D, de Pauw B, Meunier F, Marinus A, Collette L, Sylvester R, Meis J, Boogaerts M, Selleslag D, Krcmery V, von Sinner W, MacDonald P, Doyen C, Vandercam B.** 1998. An EORTC international multicenter randomized trial (EORTC number 19923) comparing two dosages of liposomal amphotericin B for treatment of invasive aspergillosis. Clinical infectious diseases : an official publication of the Infectious Diseases Society of America **27:**1406-1412.
3. **Walsh TJ, Goodman JL, Pappas P, Bekersky I, Buell DN, Roden M, Barrett J, Anaissie EJ.** 2001. Safety, tolerance, and pharmacokinetics of high-dose liposomal amphotericin B (AmBisome) in patients infected with Aspergillus species and other filamentous fungi: maximum tolerated dose study. Antimicrobial agents and chemotherapy **45:**3487-3496.

4. **Shoham S, Magill SS, Merz WG, Gonzalez C, Seibel N, Buchanan WL, Knudsen TA, Sarkisova TA, Walsh TJ.** 2010. Primary treatment of zygomycosis with liposomal amphotericin B: analysis of 28 cases. Medical mycology **48:**511-517.

5. **Hong Y, Shaw PJ, Nath CE, Yadav SP, Stephen KR, Earl JW, McLachlan AJ.** 2006. Population pharmacokinetics of liposomal amphotericin B in pediatric patients with malignant diseases. Antimicrobial agents and chemotherapy **50:**935-942.

6. **Hope WW, Goodwin J, Felton TW, Ellis M, Stevens DA.** 2012. Population pharmacokinetics of conventional and intermittent dosing of liposomal amphotericin B in adults: a first critical step for rational design of innovative regimens. Antimicrobial agents and chemotherapy **56:**5303-5308.

7. **Wurthwein G, Young C, Lanvers-Kaminsky C, Hempel G, Trame MN, Schwerdtfeger R, Ostermann H, Heinz WJ, Cornely OA, Kolve H, Boos J, Silling G, Groll AH.** 2012. Population pharmacokinetics of liposomal amphotericin B and caspofungin in allogeneic hematopoietic stem cell recipients. Antimicrobial agents and chemotherapy **56:**536-543.

8. **Alak A, Moy S, Bekersky I.** 1996. A high-performance liquid chromatographic assay for the determination of amphotericin B serum concentrations after the administration of AmBisome, a liposomal amphotericin B formulation. Therapeutic drug monitoring **18:**604-609.

9. **Neely MN, van Guilder MG, Yamada WM, Schumitzky A, Jelliffe RW.** 2012. Accurate detection of outliers and subpopulations with Pmetrics, a nonparametric and parametric pharmacometric modeling and simulation package for R. Therapeutic drug monitoring **34:**467-476.

10. **D'Argenio DZ, Schumitzky A, Wang X.** 2009. ADAPT 5 user's guide: pharmacokinetic/pharmacodynamic systems analysis software. . Biomedical Simulations Resource, Los Angeles, CA.

11. **Hamill RJ, Sobel JD, El-Sadr W, Johnson PC, Graybill JR, Javaly K, Barker DE.** 2010. Comparison of 2 doses of liposomal amphotericin B and conventional amphotericin B deoxycholate for treatment of AIDS-associated acute cryptococcal meningitis: a randomized, double-blind clinical trial of efficacy and safety. Clinical infectious diseases : an official publication of the Infectious Diseases Society of America **51:**225-232.

12. **Hope WW, Castagnola E, Groll AH, Roilides E, Akova M, Arendrup MC, Arikan-Akdagli S, Bassetti M, Bille J, Cornely OA, Cuenca-Estrella M, Donnelly JP, Garbino J, Herbrecht R, Jensen HE, Kullberg BJ, Lass-Florl C, Lortholary O, Meersseman W, Petrikkos G, Richardson MD, Verweij PE, Viscoli C, Ullmann AJ, Group EFIS.** 2012. ESCMID* guideline for the diagnosis and management of Candida diseases 2012: prevention and management of invasive infections in neonates and children caused by Candida spp. Clinical microbiology and infection : the official publication of the European Society of Clinical Microbiology and Infectious Diseases **18 Suppl 7:**38-52.

13. **Walsh TJ, Anaissie EJ, Denning DW, Herbrecht R, Kontoyiannis DP, Marr KA, Morrison VA, Segal BH, Steinbach WJ, Stevens DA, van Burik JA, Wingard JR, Patterson TF, Infectious Diseases Society of A.** 2008. Treatment of aspergillosis: clinical practice guidelines of the Infectious Diseases Society of America. Clinical infectious diseases : an official publication of the Infectious Diseases Society of America **46:**327-360.

14. **Walsh TJ, Finberg RW, Arndt C, Hiemenz J, Schwartz C, Bodensteiner D, Pappas P, Seibel N, Greenberg RN, Dummer S, Schuster M, Holcenberg JS.** 1999. Liposomal amphotericin B for empirical therapy in patients with persistent fever and neutropenia. National Institute of Allergy and Infectious Diseases Mycoses Study Group. The New England journal of medicine **340:**764-771.

15. **Wasan KM, Grossie VB, Jr., Lopez-Berestein G.** 1994. Concentrations in serum and distribution in tissue of free and liposomal amphotericin B in rats during continuous intralipid infusion. Antimicrobial agents and chemotherapy **38:**2224-2226.

16. **Wasan KM, Kennedy AL, Cassidy SM, Ramaswamy M, Holtorf L, Chou JW, Pritchard PH.** 1998. Pharmacokinetics, distribution in serum lipoproteins and tissues, and renal toxicities of amphotericin B and amphotericin B lipid complex in a hypercholesterolemic rabbit model: single-dose studies. Antimicrobial agents and chemotherapy **42:**3146-3152.

17. **Wasan KM, Morton RE, Rosenblum MG, Lopez-Berestein G.** 1994. Decreased toxicity of liposomal amphotericin B due to association of amphotericin B with high-density lipoproteins: role of lipid transfer protein. Journal of pharmaceutical sciences **83:**1006-1010.

18. **Wasan KM, Rosenblum MG, Cheung L, Lopez-Berestein G.** 1994. Influence of lipoproteins on renal cytotoxicity and antifungal activity of amphotericin B. Antimicrobial agents and chemotherapy **38:**223-227.

397 Table 1 Patient demographics of cohorts undergoing sampling on day one of therapy and at
398 steady state
399

Demographic	Day one (n=35)	Steady state (n=25)
Age (μ ± SD, range; years)	8.7 ± 4.6 (1 - 17)	10.5 ± 6.6 (1 - 17)
Gender (M:F)	22:13	15:10
Weight (μ ± SD, range; kg)	26.9 ± 14.0 (8.8 - 67.5)	25.4 ± 16.2 (11.2 – 67.5)
Duration of therapy (μ ± SD, range; days)	11.9 ± 19.4 (1 - 41)	15.5 ± 11.3 (9.5 - 41)
Underlying diagnosis (no. patients)		
Hematopoietic stem cell transplant		
Leukemia	6	5
Sickle cell disease	1	1
Aplastic anemia	1	0
Chemotherapy		
Leukemia	8	5
Lymphoma	7	5

Solid tumor	7	4
HIV	4	4
Chronic granulomatous disease	1	1
Clinical syndrome (no. patients)		
Established infection	6	6
Empiric treatment	29	19
Pathogen		
Candida albicans	2	2
Candida parapsilosis	1	1
Aspergillus fumigatus	3	3
Cryptosporidium	1	1
Clinical response		
Success	29	21
Failure	8	4
Breakthrough	1	0

400

401

402 1

403 Table 2. The parameter estimates for the final 2-compartment pharmacokinetic model

Parameter	Vin (L)	Vfin (L)	Kcp(h^{-1})	Kpc(h^{-1})	K (h^{-1})	Cl (L h^{-1} 70 kg^{-1})
Base model						
Mean	4.543	n/a	0.28	0.888	n/a	0.488
Median	4.095	n/a	0.184	0.254	n/a	0.545
Standard Deviation	3.44	n/a	0.252	0.387	n/a	0.29
Error (CV%)	75.72	n/a	90.025	43.581	n/a	59.426
Selected model						
Mean	10.654	2.326	0.21	0.057	0.303	0.67
Median	7.998	2.986	0.178	0.033	0.027	0.665
Standard Deviation	1.523	0.978	0.130	0.01	0.094	0.239
Error (CV%)	14.295	42.064	61.905	17.544	31.023	35.672

404

405 CV%, coefficient of variation; Vin, initial volume of distribution; Vfin, final volume of
406 distribution; K, first-order inter-volume rate constant; Kcp/Kpc, first-order inter-
407 compartmental rate constants; Cl, clearance.

408

409

410

411

412

413

414

415 Table 3. Bootstrap estimates of the selected pharmacokinetic model

Parameter	Bootstrap		Final model	
	Mean estimate	95% CI	Mean estimate	95% CI
Vin (L)	10.677	10.646 – 10.87	10.654	10.67 – 10.87
Vfin (L)	2.345	2.181 – 3.023	2.326	2.162 – 3.01
Kcp (h^{-1})	0.311	0.127 – 0.42	0.210	0.108 – 0.388
Kpc (h^{-1})	0.057	0.043 – 0.061	0.057	0.043 – 0.061
K (h^{-1})	0.303	0.21 – 0.355	0.302	0.21 – 0.351
Cl (L h^{-1} 70 kg^{-1})	0.675	0.555 – 0.781	0.670	0.548 – 0.797

416

417

418

419 Figure 1. Concentration-time profiles for each patient on day one of therapy (n=35) and at
420 completion of therapy (n=25). Closed circles are the raw pharmacokinetic data from each
421 patient.

422

423 Figure 2. Scatter plots showing observed-versus-predicted values for population
424 pharmacokinetic models after the Bayesian step with a standard 2-compartment model (A)
425 and selected model (B). Open circles, dashed lines and solid lines represent individual

observed-predicted data points, line of identity, and the linear regression of observed-predicted values, respectively.

Figure 3. Concentration-time profiles for two patients receiving LAmB (10 mg kg^{-1}). Initial (Vin) and final (Vfin) estimates for volume of distribution (Vd) are shown. Open circles and solid lines represent the raw data and simulated concentration-time profiles for each patient, respectively. Patient A exhibits evolving PK with a contraction in the Vd while patient B exhibits stable Vd.

Figure 4 Comparisons of dose-normalised Cmax (A) and AUC_{0-24} (B) at steady state with respect to dose per unit weight. Solid and dashed lines represent linear regression and 95% confidence intervals, respectively.

Figure 5. Relationship between Bayesian estimates of AUC_{0-24} at steady state with respect to change in serum creatinine. Solid and dashed lines represent linear regression and 95% confidence intervals, respectively.

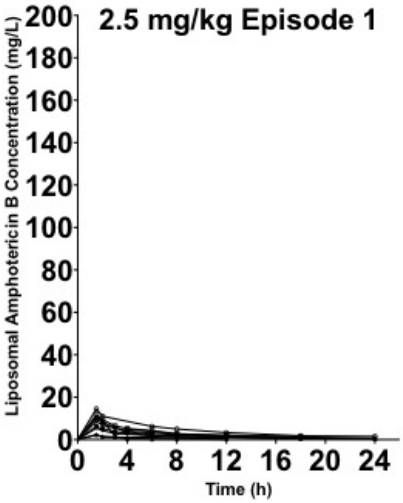
2.5 mg/kg Episode 1
Liposomal Amphotericin B Concentration (mg/L)
Time (h)

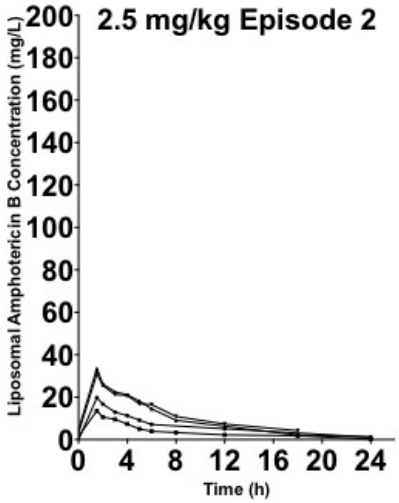
2.5 mg/kg Episode 2
Liposomal Amphotericin B Concentration (mg/L)
Time (h)

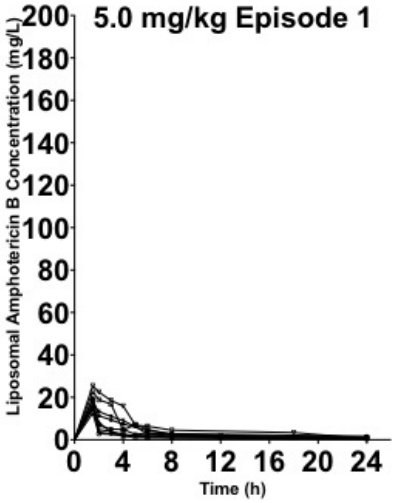
5.0 mg/kg Episode 1
Liposomal Amphotericin B Concentration (mg/L)
Time (h)

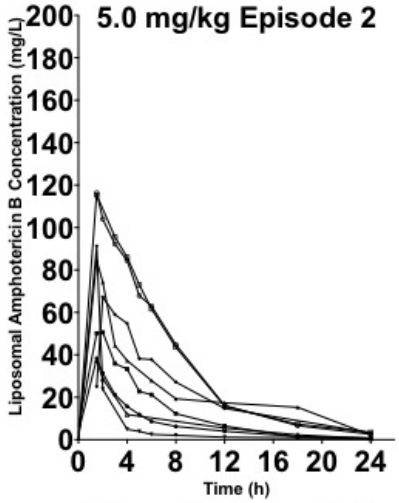
5.0 mg/kg Episode 2
Liposomal Amphotericin B Concentration (mg/L)
Time (h)

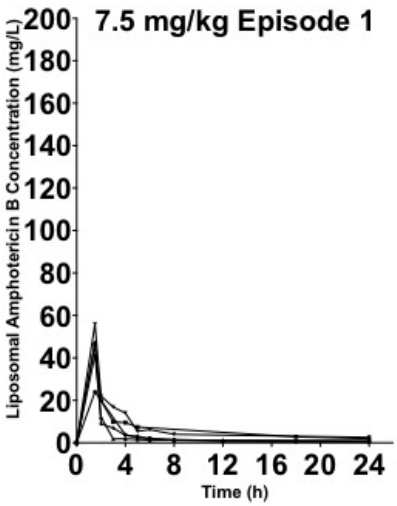
7.5 mg/kg Episode 1
Liposomal Amphotericin B Concentration (mg/L)
Time (h)

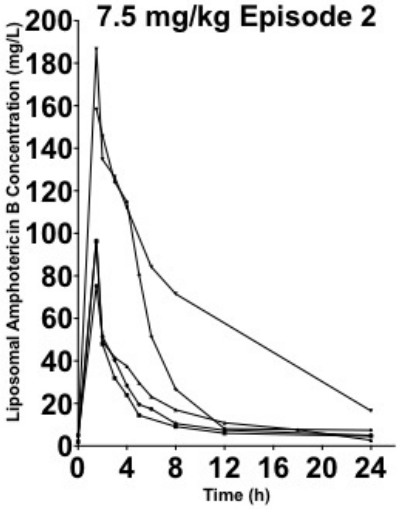
7.5 mg/kg Episode 2
Liposomal Amphotericin B Concentration (mg/L)
Time (h)

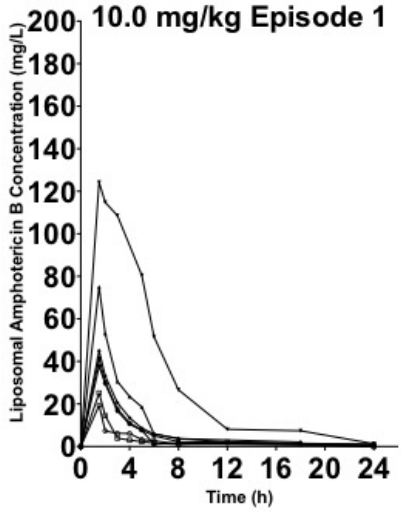
10.0 mg/kg Episode 1
Liposomal Amphotericin B Concentration (mg/L)
Time (h)

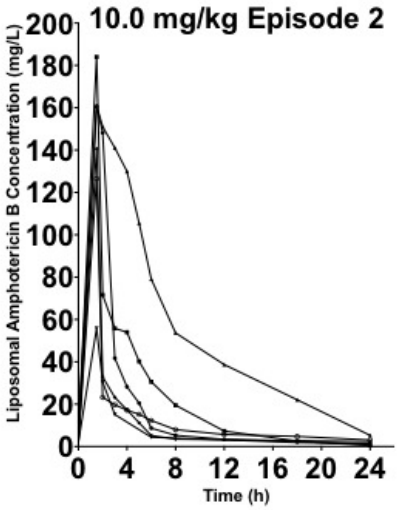
10.0 mg/kg Episode 2
Liposomal Amphotericin B Concentration (mg/L)
Time (h)

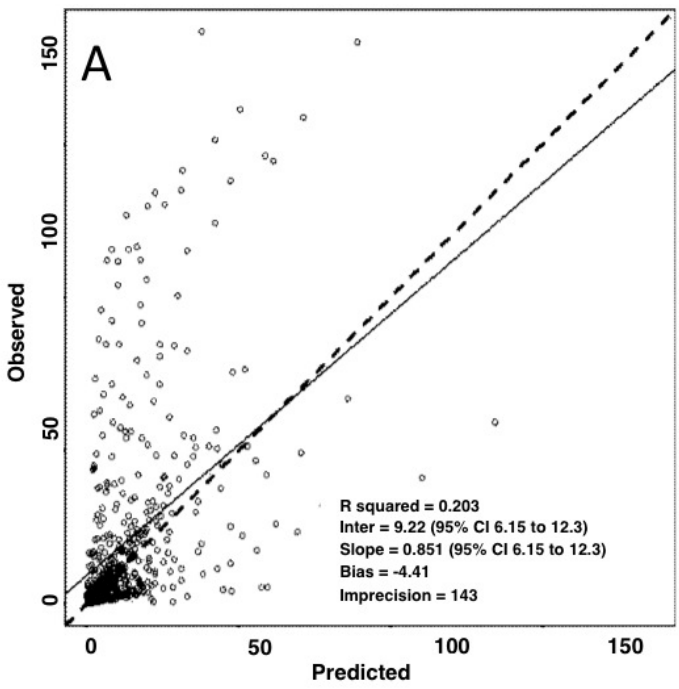
A
Observed
Predicted
0
50
100
150
R squared = 0.203
Inter = 9.22 (95% CI 6.15 to 12.3)
Slope = 0.851 (95% CI 6.15 to 12.3)
Bias = -4.41
Imprecision = 143

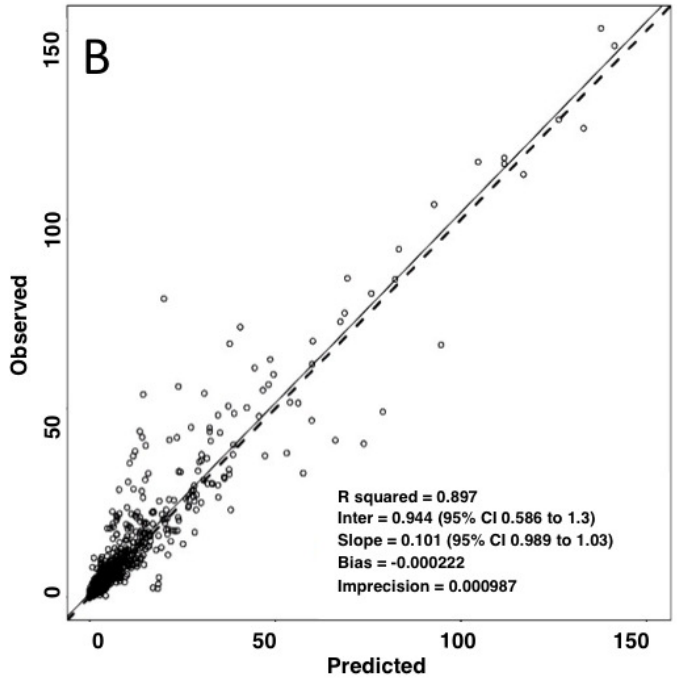
B
Observed
Predicted
0
50
100
150
R squared = 0.897
Inter = 0.944 (95% CI 0.586 to 1.3)
Slope = 0.101 (95% CI 0.989 to 1.03)
Bias = -0.000222
Imprecision = 0.000987

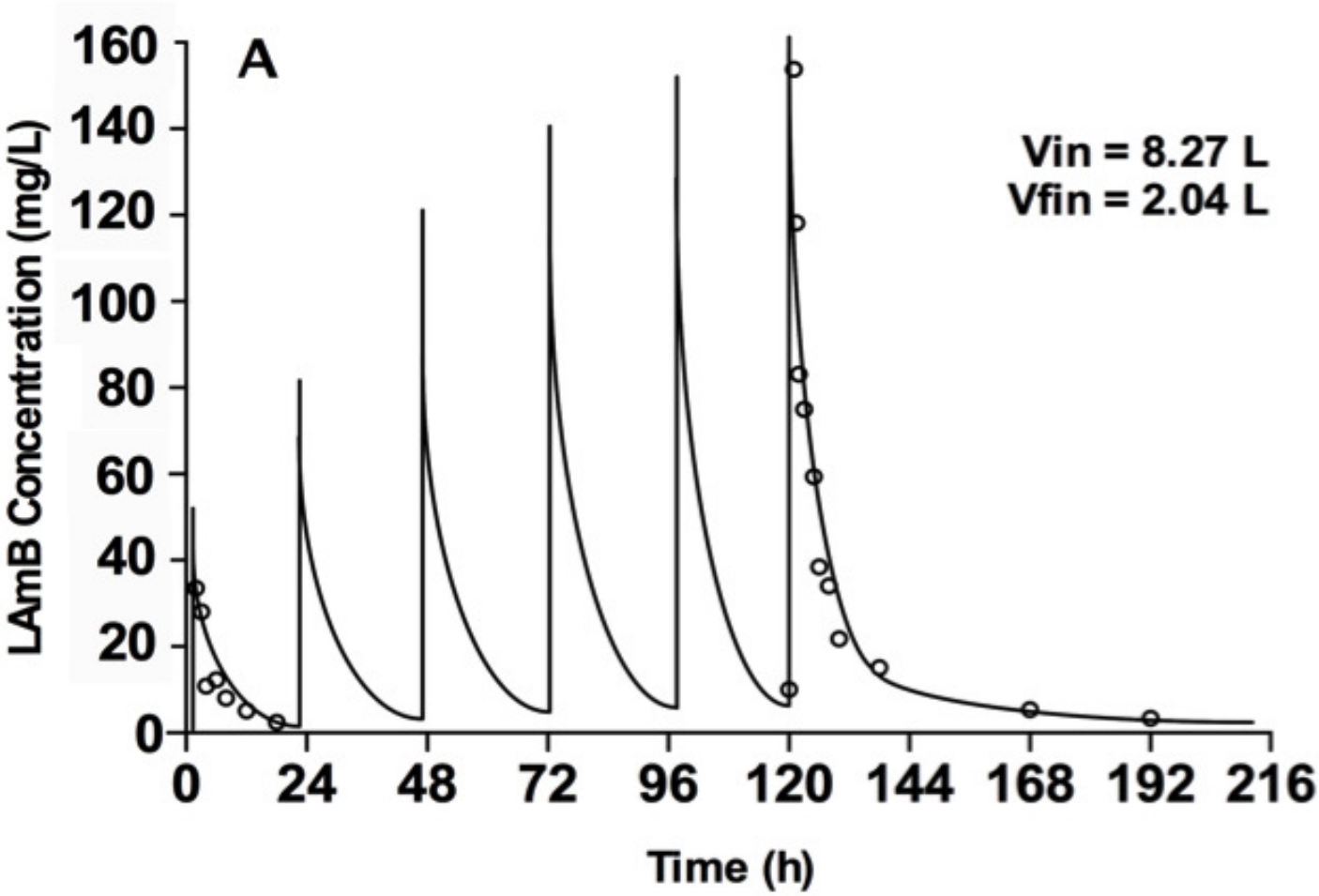
A
Vin = 8.27 L
Vfin = 2.04 L
LAmB Concentration (mg/L)
160
140
120
100
80
60
40
20
0
0
24
48
72
96
120
144
168
192
216
Time (h)

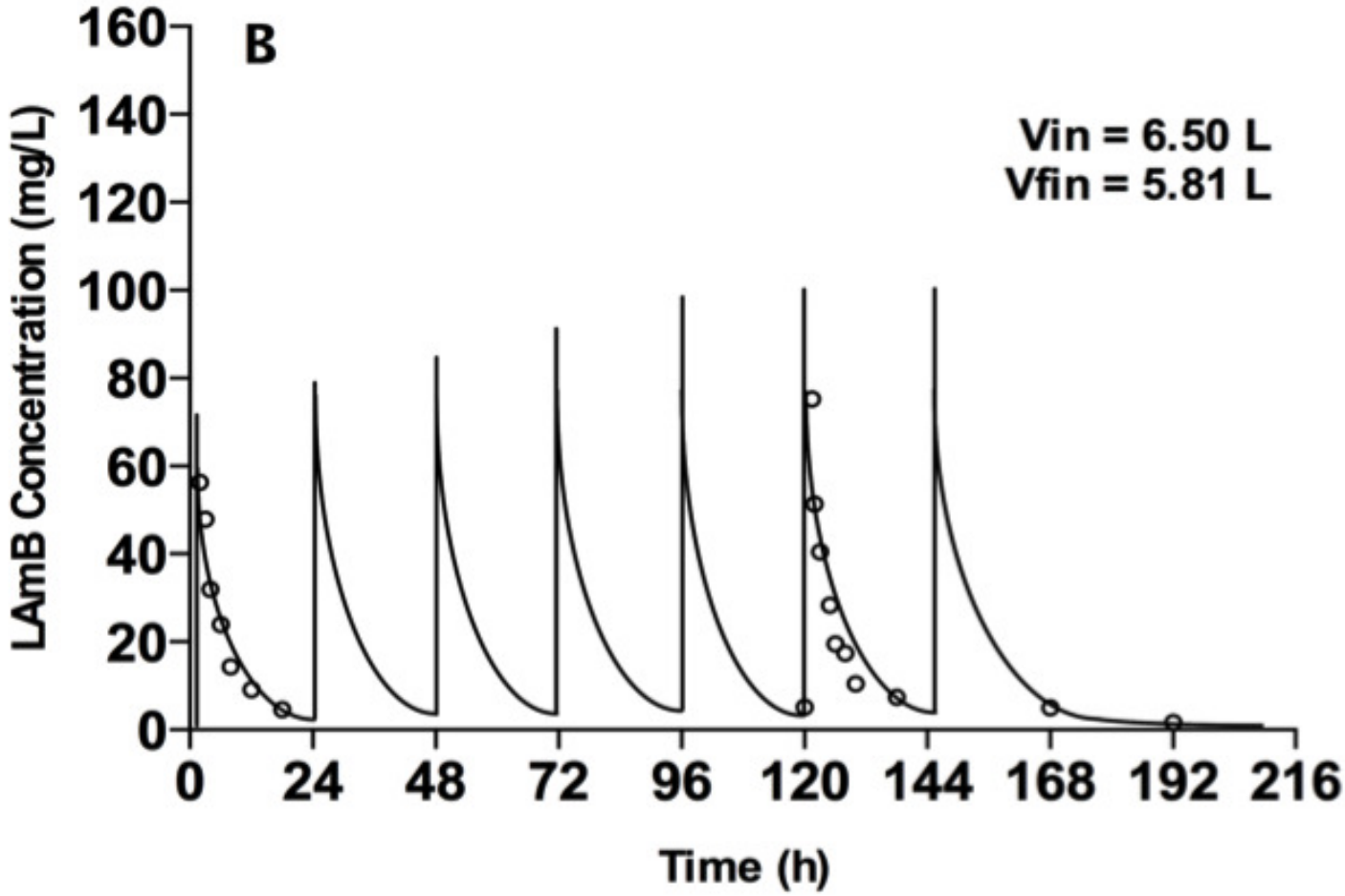
B
Vin = 6.50 L
Vfin = 5.81 L
LAmB Concentration (mg/L)
160
140
120
100
80
60
40
20
0
0
24
48
72
96
120
144
168
192
216
Time (h)

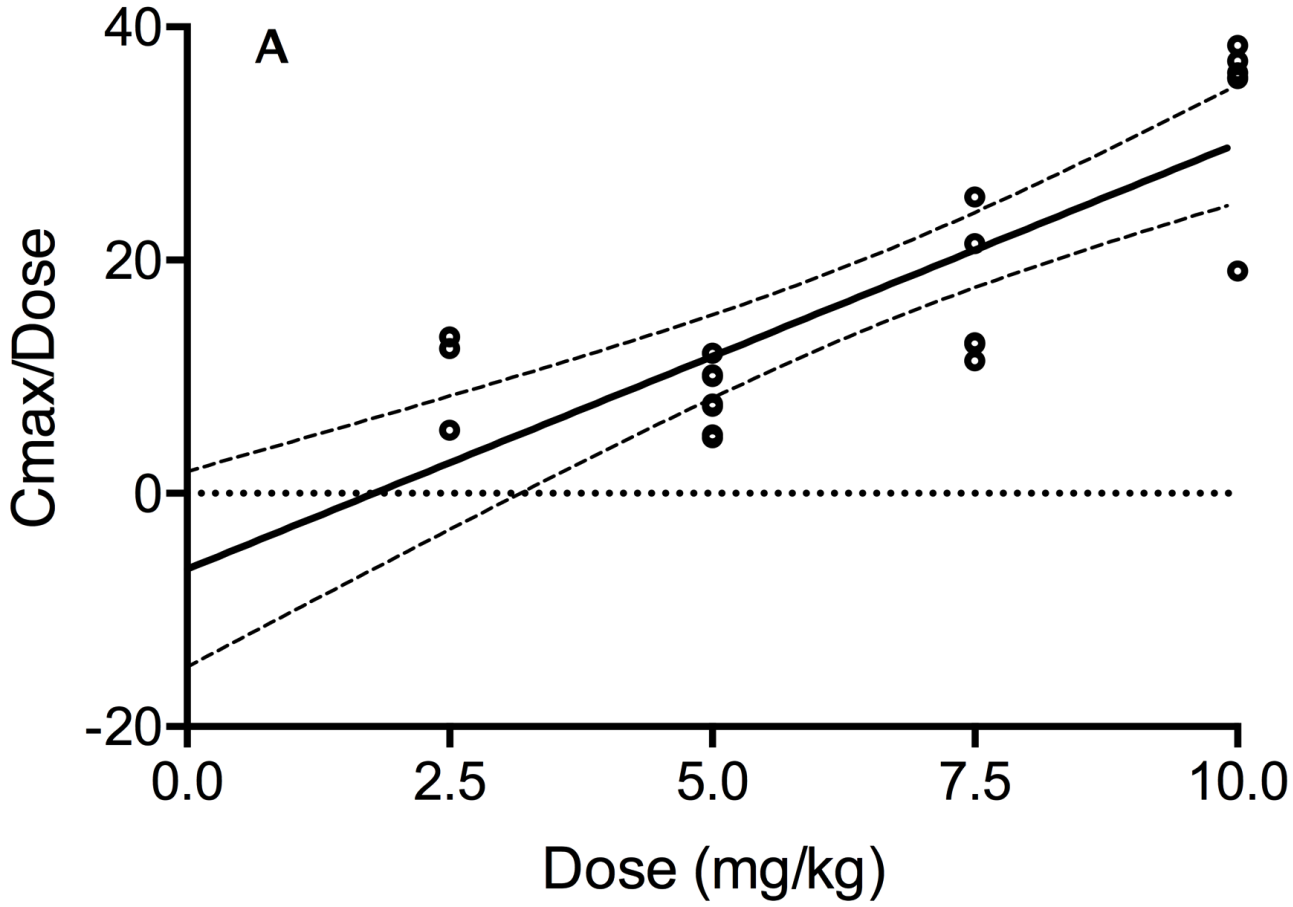
A
40
20
0
-20
Cmax/Dose
0.0
2.5
5.0
7.5
10.0
Dose (mg/kg)

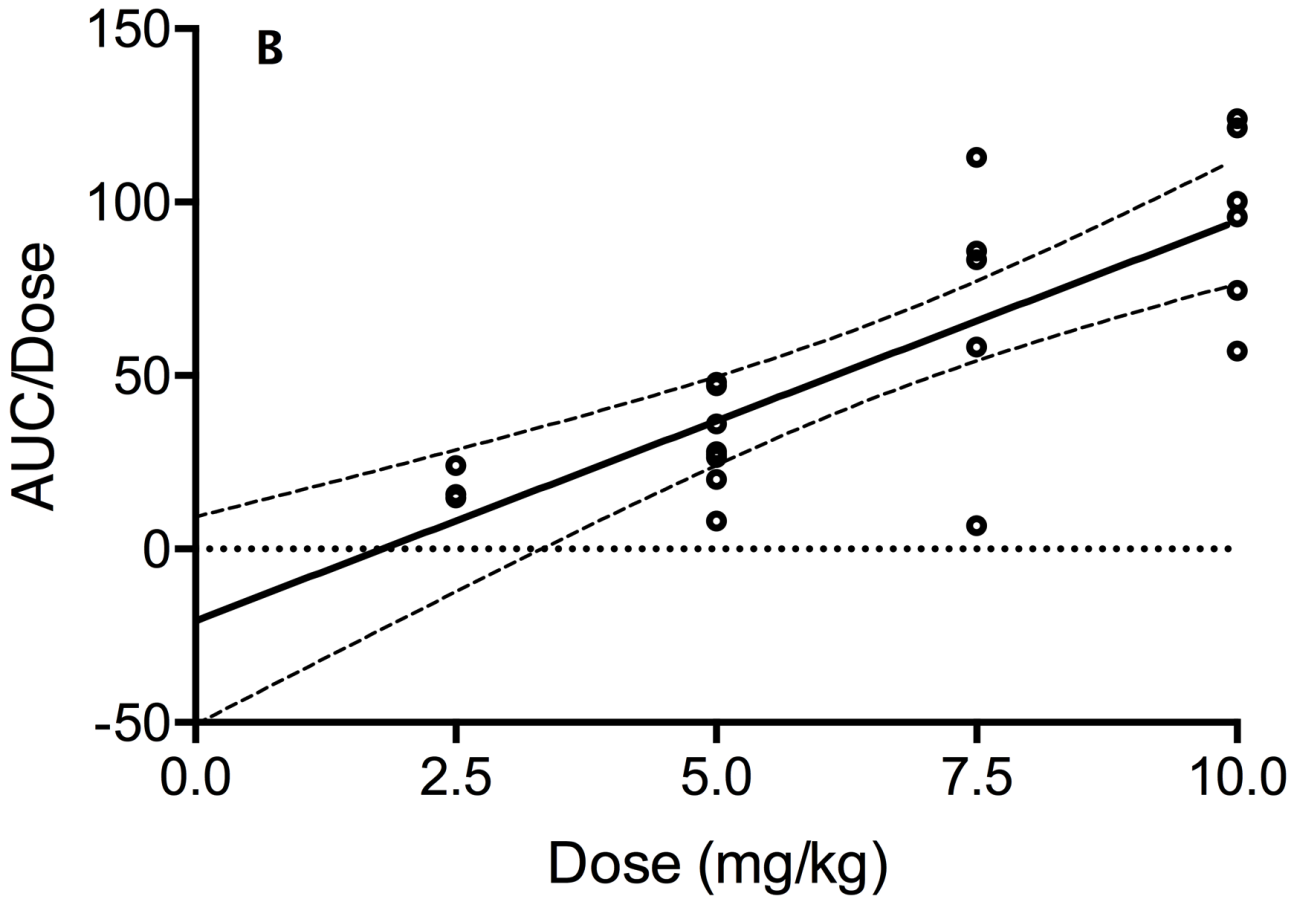
B
150
100
50
0
-50
AUC/Dose
0.0
2.5
5.0
7.5
10.0
Dose (mg/kg)

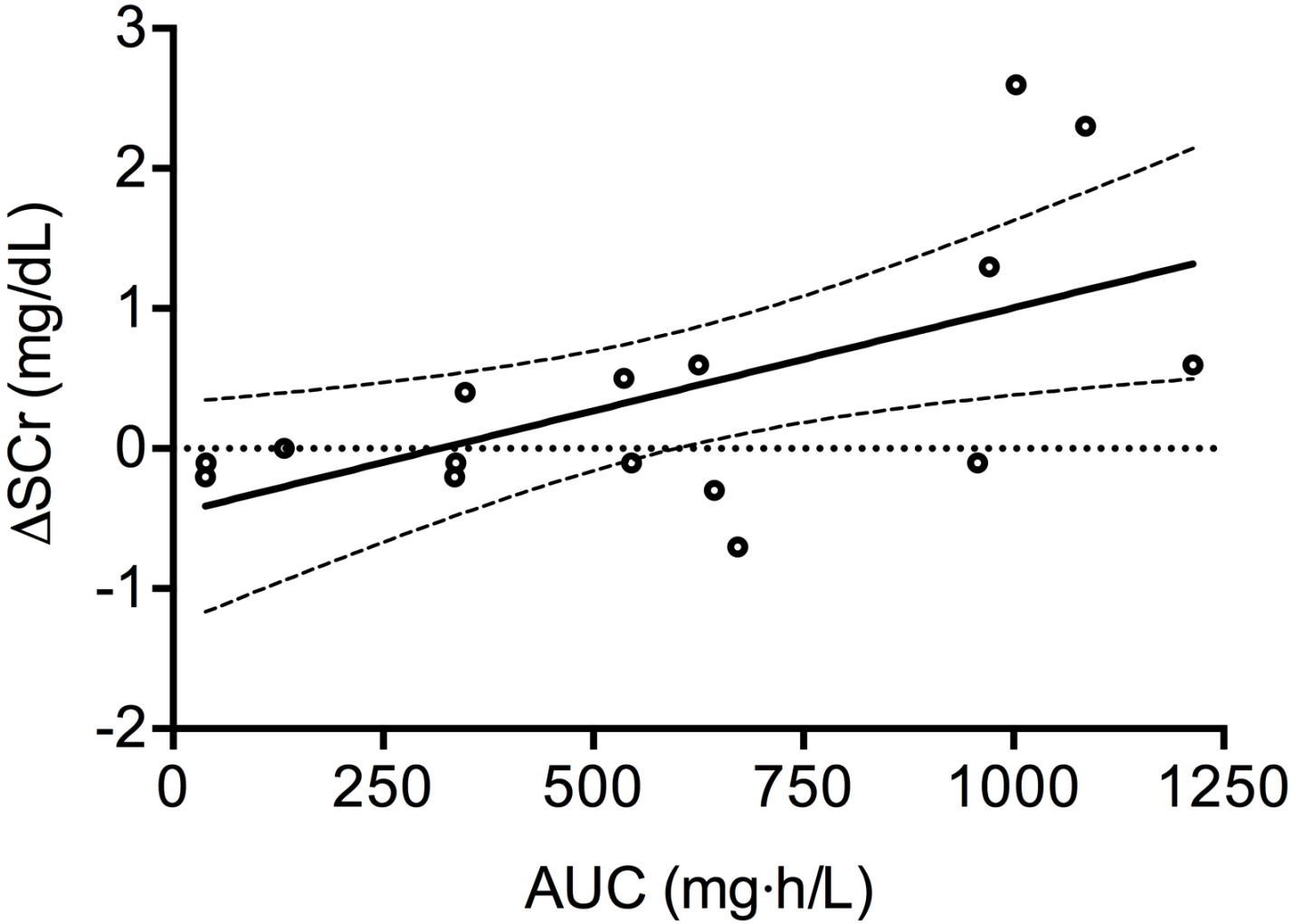
3
2
1
0
-1
-2
ΔSCr (mg/dL)
0
250
500
750
1000
1250
AUC (mg·h/L)